J. Condensed Matter Nucl. Sci. 4 (2011) 45-55

Research Article

Measurements of Excess Power Effects In Pd/D_2O Systems Using a New Isoperibolic Calorimeter

M.H. Miles *
Dixie State College, St. George, UT 84770, USA

M. Fleischmann
Bury Lodge, Duck Street, Tisbury, Salisbury, Wilts SP3 6LJ, UK

Abstract

Relatively inexpensive isoperibolic calorimeters have been designed and constructed with the goal of obtaining a constant heat transfer coefficient that is insensitive to normal changes in the electrolyte level during electrolysis. Four prototypes were constructed from copper tubing and used different insulating materials. Preliminary tests on two of these new calorimeters show excellent stability for the cell temperature measurements, stable heat transfer coefficients during electrolysis, and precise power measurements. Initial applications include nitrate electrolytes and co-deposition systems. There was no evidence for any shuttle reactions in these experiments.

Keywords: Co-deposition, Electrolysis, Heat capacity, Heat conduction, Nitrates, Shuttle reactions, Temperature, Thermistors

1. Introduction: Design Considerations

An important goal for isoperibolic calorimeters is a constant heat transfer coefficient that does not change as the electrolyte level decreases due to the electrolysis and evaporation. All measurements could then be evaluated with a single, predetermined value for the heat transfer coefficient. The placement of the thermistors in a secondary compartment outside the cell has been shown to minimize the cell electrolyte level effect [1–4]. This type of calorimeter can then be modeled as a fluid in which the electrochemical cell serves as a heating element for the substance in the adjacent compartment.

The size of the calorimetric system must be carefully considered in the design. Large systems give slower electrolyte level changes along with larger heat capacities and time constants. Small calorimetric cells yield faster electrolyte level changes and smaller heat capacities and time constants, but their small cell volumes require more frequent makeup of H_2O or D_2O additions. The heat transfer coefficient will also increase with the surface area of the calorimetric system.

*E-mail: melmiles1@juno.com

Adequate stirring of the cell contents by the electrolysis gases requires thin, tall cells where the cell diameter does not exceed 3 or 4 cm. All these factors were carefully considered in selecting design features for these new isoperibolic calorimeters.

Desired features of isoperibolic calorimeters include simple construction and low costs, heat transfer mainly by either conduction or by radiation (Dewar type), and a wide dynamic range from 20°C to boiling for the cell temperature with cell input power levels ranging from 0 to 10 W. This requires heat transfer coefficients near $k_C = 0.13$ W/K if the heat transfer is by conduction or near $k_R = 0.83 \times 10^{-9} W/K^4$ if the heat transfer is by radiation (Dewar). Because of the simpler construction and lower costs, isoperibolic calorimeters providing heat transfer by conduction were selected rather than Dewar cells. It should be noted, however, that a Dewar design fitted with a metallic conductive cylinder insert containing two thermistors and the glass electrochemical cell has also been proposed (see Fig. A.27 of Ref. [5]). Although this calorimetric design has never been constructed, it would likely have provided a constant radiative heat transfer coefficient that would be independent of the electrolyte level (p. 26 of Ref. [5]).

2. Experimental Details of the Calorimetric Design

Four prototype isoperibolic calorimeters (A, B, C, and D) have been constructed from commercial copper tubing and copper end caps, and two (A, B) have been tested. Each calorimeter consisted of two completely isolated copper cylinders. The outer copper cylinder for each calorimeter had a 5.1 cm (2.0 in) diameter and a 28 cm height. The inner copper cylinder (3.2 cm ×20 cm) was completely separated from the outer cylinder by the insulating material consisting of either pipe foam insulation (Cell A) or of tightly packed Oregon timber sawdust (Cell B). The glass electrochemical cell (2.5 cm × 20 cm) was a large commercial glass test tube (Kimax). This test tube cell was positioned inside the inner copper cylinder and filled 2/3 full using 50.0 mL of the selected electrolyte. Two thermistors were positioned on opposite sides of the outer wall of the glass tube with each thermistor level with the center of the cathode used. Thermal contact between the glass cell and the inner copper tube was provided by Mobil-1 (5–30 W) synthetic motor oil (50 mL) as the heat conducting fluid. The Mobil-1 oil has a reported density of 0.80 g/mL at 15°C and a heat capacity of 210 J/g K at 80°C. This 50 mL of Mobil-1 oil filled the secondary chamber well above the cell electrolyte level. It is expected that this calorimetric design will provide for high cell operating temperatures up to the boiling point of the selected electrolyte solution.

3. Review of Equations for Isoperibolic Calorimetry

The mathematical equations that model isoperibolic calorimetry have been presented elsewhere [5–8], thus this will only be a brief review. Full details are given in Appendix A1. The fundamental modeling equation is

$$P_{\text{calor}} = P_{\text{EI}} + P_{\text{H}} + P_{\text{X}} + P_{\text{C}} + P_{\text{R}} + P_{\text{gas}} + P_{\text{W}}, \tag{1}$$

where these individual power terms have all been defined elsewhere [5–8] as well as in Appendix A2. Equation (1) represents a differential equation because

$$P_{\text{calor}} = C_{\text{p}} M \, \text{d}T/\text{d}t, \tag{2}$$

where $C_{\text{p}}M$ (J/K) is the heat capacity of the calorimetric system consisting of the molar heat capacity (C_{p}) of H_2O or D_2O in J/K mol and the number of equivalent moles (M) of the H_2O or D_2O that would yield this heat capacity.

It is useful in initial calculations to assume that there is no anomalous excess power, $P_X = 0$, thus Eq. (1) becomes

$$P_{\text{calor}} = P_{\text{EI}} + P_{\text{H}} + 0 + P'_{\text{C}} + P_{\text{R}} + P_{\text{gas}} + P_{\text{W}}. \tag{3}$$

The simple subtraction of Eq. (3) from Eq. (1) yields

$$0 = P_{\text{X}} + P_{\text{C}} - P'_{\text{C}} = P_{\text{X}} - k_{\text{C}} \Delta T + k'_{\text{C}} \Delta T \tag{4}$$

or

$$P_X = (k_C - k'_C)\Delta T, \tag{5}$$

where $\Delta T = T - T_b$. Therefore, the difference between the true conductive heat transfer coefficient (k_C) and the pseudo-heat transfer coefficient (k'_C) obtained by assuming $P_X = 0$ provides for a simple calculation of the actual excess power via Eq. (5). All of the power terms in Eq. (1), however, should be considered in the determination of k'_C.

4. Experimental Results

The use of this new isoperibolic calorimetric design requires the evaluation of the conductive heat transfer coefficient, k_C, and the heat capacity, C_pM, of the calorimetric system (see Appendix A1). Several experiments using H_2O control electrolytes yielded $k_C = 0.164$ W/K for Cell A and $k_C = 0.133$ W/K for Cell B.

These cells differ only by the use of foam insulation in Cell A and packed sawdust insulation in Cell B.

4.1. Heat capacity/differential and integral equations

The experimental cooling curve obtained by simply turning off the cell current provides a convenient method for determining the heat capacity, C_pM, of the calorimetric system. For a H_2O control experiment at zero current, Eq. (1) becomes

$$C_pM\, dT/dt = -k_C(T - T_b). \tag{6}$$

This differential equation can be rearranged to

$$dT/(T - T_b) = -(k_C/C_pM)dt \tag{7}$$

and then integrated to yield

$$-\ln(T - T_b)/(T_0 - T_b) = (k_C/C_pM)t. \tag{8}$$

This integrated equation is of the form $y = mx$ where the slope (m) is given by $m = k_C/C_pM$.

The experimental cooling curve for Cell B using a H_2O control is present in Fig. 1, where T_2 is the cell temperature measured by thermistor 2. This figure shows the expected exponential decrease of $T_2 - T_b$ with time. Figure 2 shows the same data using the integrated Eq. (8). The slope $m = 0.01752\,\text{min}^{-1} = 2.920 \times 10^{-4}\text{s}^{-1}$. Therefore $C_pM = k_C/m = 456$ J/K. The water equivalent that would give this same heat capacity is 6.06 mol ($C_p = 75.291$ J/mol K for H_2O). The heat capacity of the system can also be calculated using the differential equation (Eq. (6)) directly, but this is considerably less accurate because of the estimate of dT/dt. From Eq. (6), $C_pM = -k_C(T - T_b)/dT/dt)$. Table 1 presents the value for C_pM obtained directly from Fig. 1 at 10, 30, and 65 min. The three values calculated for C_pM range from 427 to 485 J/K with a mean of 457±29 J/K. It is obvious that more accurate results for C_pM are obtained by use of the integrated equation (Eq. (8)) where the results can be displayed in a straight line form (Fig. 2). The same is true for all isoperibolic calorimetric results using Eq. (1). Numerical integration of the experimental calorimetric data along with casting them into the straight line form, $y = mx + b$, gives the most accurate results as previously reported [5–9].

The time constants for Cells A and B can be readily calculated once k_C and C_pM are known because $\tau = C_pM/k_C$. This yields $\tau = 3420$ s or 57 min for Cell B and 46 min for Cell A.

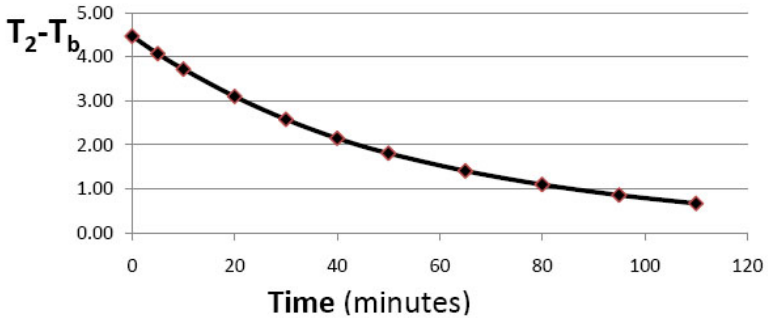

Figure 1. Experimental cooling curve for Cell B.

4.2. Estimated heat capacity

The heat capacity of the cell can also be estimated by considering the heat capacity of all materials in the cell or in contact with the cell that undergo the same temperature changes. These calculations give 208 J/K for the 50.0 mL of H_2O used, 133 J/K for the 344 g of the inner copper cylinder, 84 J/K for 50 mL of Mobil-1 oil, 31 J/K for 42 g of the glass cell, and 2 J/K for the copper cathode, platinum wire, palladium and nickel present. The calculated total of 458 J/K is close to the measured value for C_pM. For a cell filled with 50.0 mL of D_2O giving 233 J/K, the calculated total for C_pM would be 483 J/K. Methods for minimizing the effect of errors for C_pM have been previously presented [3,7].

4.3. Detection of "Heat After Death" effects

It should be noted that cooling curves such as Figs. 1 and 2 provide a useful method for determining lingering excess power effects or "heat-after-death" when electrolysis ceases in active D_2O/Pd experiments. Cell cooling that departs from Eq. (8) or Fig. 2 would be readily apparent. Such studies of cooling curve behavior are planned for future D_2O/Pd experiments. A previous study of Pd-B/D_2O in a Dewar type cell showed marked deviations from the expected cooling curve behavior (see pp. 22–23 and Figs. A.23 and A.24 of Ref. [5]). For heat transfer by radiation with no excess power present, Eq. (1) becomes

$$C_pM\mathrm{d}T/\mathrm{d}t = -k_R(T^4 - T_b^4), \tag{9}$$

Table 1. Heat capacity (C_pM) for Cell B calculated from the cooling Curve of Fig. 1 using the differential equation (Eq. (8)).

T (min)	$\mathrm{d}T_{cell}/\mathrm{dt}$ (K/min)	$T-T_b$(K)	C_pM (J/K)
10	-10.8×10^{-4}	3.72	458
30	-8.03×10^{-4}	2.58	427
65	-3.87×10^{-4}	1.41	485
Mean $C_pM = 457 \pm 29$ J/K			

when the current is off. The rearrangement and integration of this differential equation yields

$$\ln(T + T_b)(T_o - T_b)/(T_o + T_b)(T - T_b) + 2\tan^{-1}(T/T_b) - 2\tan^{-1}(T_o/T_b) = 4T_b^3 k_R t/C_p M. \quad (10)$$

Although more complicated than Eq. (8) for heat transfer by conduction, the use of Eq. (10) for Dewar cells in a previous Pd-B study readily shows the presence of the "heat-after-death" effect [5].

4.4. Experimental Tests for Shuttle Reactions

Potassium nitrate (KNO_3) has been widely used for years by electrochemists as an inert supporting electrolyte. However, it has been proposed that shuttle reactions involving nitrates may give false excess power effects [10]. Theoretically, the nitrate ion may be reduced at the cathode to form various gaseous nitrogen oxides, nitrite ions (NO_2^-), or even N_2 or NH_4^+. With the use of special electrocatalyts and conditions, some electrochemical reduction of nitrates is possible [11]. In molten nitrates ($LiNO_3$–KNO_3) at elevated temperatures (250°C), there exists a large 4.5 V electrostability region between the reduction of lithium ions and the oxidation of nitrate ions [12,13]. This demonstrates the stability of the nitrate ion even at high temperatures. The anodic limit for the nitrate melt is the oxidation of the nitrate ion, $NO_3^- \rightarrow NO + O_2 + e^-$, followed by the further reaction of NO with oxygen to form brown NO_2 gas [12].

Because of the proposed shuttle reactions involving nitrates [10], an initial study using this new isoperibolic calorimeter was the investigation of 0.154 M KNO_3 in Cell B. This study used a platinum wire cathode (1 mm × 15 mm) and a platinum coil anode. The H_2O + 0.154 M KNO_3/Pt system was investigated over several days of electrolysis at currents of 80, 100, and 150 mA. These were no measurable excess power effects. The correct value of $k'_C = 0.133$ W/K was obtained using Cell B and assuming $P_X = 0$. Therefore k_C–$k'_C = 0$ and $P_X = 0$ from Eq. (5). Recent cyclic voltammetric studies on KNO_3+$NaNO_2$ have confirmed that there are no reversible reactions involving nitrates or nitrites that could act as shuttle reactions.

The measured pH of the 0.154 M KNO_3 solution, however, changed from near neutral initially (pH = 7.02) to pH = 10.24 at the end of this study. Any electrochemical reaction of NO_3^- ions to form a neutral product such as NO_2, NO or N_2 results in the production of OH^-ions to maintain electroneutrality. For the total of 27,626 C used in this study, the observed pH change could be explained by 0.003% of the current being consumed by the reaction of NO_3^- to form a neutral product. The remaining 99.997% of the current was apparently consumed by the expected H_2O electrolysis. The electrochemical reaction of nitrates would, therefore, change the thermoneutral potential (E_H)

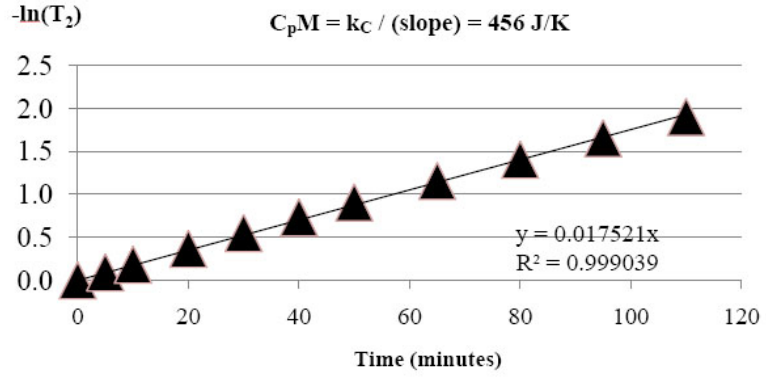

Figure 2. Cooling curve data of Fig. 1 using the integrated equation where $-\ln(T_2)$ represents the left-hand side of Eq. (8).

by only 4.4 $\times 10^{-5}$ V. At the highest current used (150 mA), this nitrate reaction would give a calorimetric error of $(4.4 \times 10^{-5}\ \text{V})(0.150\ \text{A}) = 6.6 \times 10^{-6}$ W or less than 0.007 mW. Therefore, based on this study of 0.154 M KNO_3/Pt, the use of KNO_3 as an inert electrolyte in calorimetric studies would be justified. In a related experiment using 0.158 M KNO_3+0.0577 M $NaNO_2$, 99.992% of the current (90,720 C) was consumed by H_2O electrolysis. There are no shuttle reactions involving nitrates or nitrites that would give a false excess power effect. In both experiments, the volume of H_2O consumed was larger than the theoretical amount based on Faraday's law, and this provides further evidence against shuttle reactions.

4.5. Co-deposition/light water controls

This new calorimeter was also used to study the 0.15 M NH_4Cl + 0.15 M NH_4OH + 0.025 M $PdCl_2$ co-deposition system in H_2O. Complete results are given elsewhere [14]. In this case, a chemical excess power effect was detected early in the experiment due to the solution becoming acidic (pH = 1.25) resulting in chlorine evolution and the formation of nitrogen trichloride (NCl_3). Similar excess power effects were measured by the Naval Research Laboratory (NRL) for this same system using a Seebeck calorimeter [15]. With further electrolysis, the solution becomes more basic, chlorine evolution ceases, the NCl_3 dissipates, and normal calorimetric results are observed [14].

In a new study, NH_4Cl + NH_4OH + $PdCl_2$ co-deposition was repeated, but following the palladium co-deposition onto a copper cathode, sufficient LiOH was added to maintain a basic pH. This provided a very stable electrolysis system with no chlorine or NCl_3 formation. The electrolysis of this system using a high current of 400 mA gave evidence for a stable cell constant that was independent of the electrolyte level. The results for this study in Cell B are given in Table 2. The mean cell constant over almost 5 h of electrolysis was $\langle k_2 \rangle = 0.1324 \pm 0.000069$ W/K. The cell constants never varied by more than ± 0.0001 W/K from the mean value. This is the best evidence to date for an isoperibolic calorimetric cell where the electrolyte level does not affect the cell constant. We were, therefore, successful in attaining our major goal for this new isoperibolic calorimeter.

Table 2. Calorimetric data summary for Cell B with I = 400 mA using the $PdCl_2$ + NH_4Cl + NH_4OH + LiOH electrolyte.

Time	$-E_{\text{cell}}$ (V)	P_{EI} (W)	ΔT_2 (K)	k_2 (W/K)
2:29	5.122	1.4564	11.000	0.1324
2:44	5.121	1.4560	10.995	0.1324
4:01	5.110	1.4516	10.970	0.1323
4:53	5.103	1.4488	10.935	0.1325
5:51	5.094	1.4452	10.915	0.1324
6:46	5.088	1.4428	10.900	0.1324
7:19	5.083	1.4408	10.890	0.1323

The change in the cell voltage with time (t, min) in Table 2 gives the linear relationship $E_{\text{cell}} = -5.122458 + 1.36 \times 10^{-4} t\ (R_2 = 0.9988)$. This is the expected behavior for water electrolysis if there are no shuttle reactions or anomalous F–P effects. The steady electrolysis of water at constant current gradually increases the electrolyte concentration and decreases the IR (resistive heating) component of the cell voltage. The changes in both P_{EI} and ΔT_2 (Table 2) are directly related to the changes in E_{cell} when there are no anomalous effects.

4.6. Co-deposition/heavy water studies

Two calorimetric studies of co-deposition have been completed using heavy water and deuterated compounds. Chlorine evolution and the related NCl_3 formation were avoided by the use of $PdCl_2 + ND_4Cl + ND_4OD + LiOD/D_2O$ similar to the very stable H_2O study shown in Table 2. Excess power effects were measured in both experiments using an electrolysis current of 100 mA. For example, $k'_C = 0.09585$ W/K with $\Delta T = 2.15$ K, thus from Eq. (5), $P_X = 80$ mW. Typically, the excess power ranged from 75 to 105 mW in both experiments. However, the excess power gradually decreased to near zero in both experiments after several days of electrolysis. It was later found that the deposited palladium had become detached from the copper cathode substrate and fell to the bottom of the cell in both experiments resulting in the palladium becoming electrochemically isolated. New experiments are planned where the copper cathode will be positioned close to the cell bottom, thus any detached palladium will remain in electrical contact with the cathode.

5. Summary of Results

New isoperibolic calorimeters that are relatively inexpensive have been designed, constructed, and tested using several different electrolyte systems. These calorimeters show stable heat transfer coefficients that do not change during electrolysis at high cell currents over long time periods. Initial studies have shown excess power effects for the $ND_4Cl + ND_4OD + PdCl_2 + LiOD/D_2O$ co-deposition system. No excess power was measured in the corresponding H_2O control study.

Shuttle reactions have been proposed by NRL as an explanation for excess power in co-deposition systems [10]. In our studies, neither calorimetric nor electrochemical measurements have detected any shuttle reactions involving nitrates or nitrites. Similar results were obtained in studies of chlorates [14]. Furthermore, no excess power was observed for the $NH_4Cl + NH_4OH + PdCl_2 + LiOH/H_2O$ control co-deposition system. Another paper in preparation [16] will focus on co-deposition experiments and the absence of any experimental evidence for the shuttle reaction hypothesis for excess power in co-deposition systems.

Acknowledgements

Financial help in the design and construction of these new calorimeters is acknowledged by M.H.M. from an anonymous fund at the Denver Foundation via Dixie State College. Steve Tetz of Wolf Creek, Oregon performed the actual construction of the four calorimetric cells. Portions of this work were presented at ICCF-15 in Rome, Italy [17].

Appendix A1. Calorimetric Equations

Treating the isoperibolic calorimetric cell as the system of interest, the First Law of Thermodynamics expressed as power (J/s or W) becomes

$$P_{calor}(t) = P_{EI}(t) + P_H(t) + P_X(t) + P_{gas}(t) + P_R(t) + P_C(t) + P_W(t). \quad (A.1)$$

By definition, P_{calor} is the power for the calorimetric cell, P_{EI} the electrochemical power, P_H the internal heater power, P_X any anomalous excess power, P_{gas} the power carried away by the gas stream exiting the open cell (D_2, O_2, D_2O vapor), P_R the net power transferred by radiation between the cell and water bath, P_C is the power transferred by conduction, and P_W represents the rate of pressure–volume work by the generated electrolysis gases (D_2, O_2). Because both the cell temperature and cell voltage change with time during electrolysis, most of the terms in Eq. (A.1) also vary with the time (t). The internal heater power, P_H, will be zero except for the time period between turning the heater on (t_1) and off (t_2). Typical values for P_H, when on, are either 0.2000 W or 0.2500 W. There are often time periods where P_X is zero or constant. As usual in thermodynamics, positive quantities represent power added to the system (calorimetric cell) and negative quantities represent power given off by the system to the surroundings.

The mathematical expressions for the terms in Eq. (A.1) are as follows:

$$P_{\text{calor}} = C_{\text{p}} M(\text{d}T/\text{d}t), \tag{A.2}$$

$$P_{\text{EI}} = (E - E_{\text{H}})I, \tag{A.3}$$

$$P_{\text{gas}} = -(I/F)\{[0.5C_{\text{P,D}_2} + 0.25C_{\text{P,O}_2} + 0.75(\mathbf{P}/(\mathbf{P}^* - \mathbf{P}))C_{\mathbf{P},\text{D}_2\text{O(g)}}]\Delta T + 0.75(\mathbf{P}/(\mathbf{P}^*\text{–}\mathbf{P}))L\}, \text{ where } \Delta T = T - T_{\text{b}}, \tag{A.4}$$

$$P_{\text{R}} = -k_{\text{R}} f(T), \text{ where } f(T) = T^4\text{–}T_{\text{b}}^4, \tag{A.5}$$

$$P_{\text{C}} = -k_{\text{C}}(T\text{–}T_{\text{b}}), \tag{A.6}$$

$$P_{\text{W}} = -RT(\text{d}n_{\text{g}}/\text{d}t) = -RT(0.75I/F). \tag{A.7}$$

For this new isoperibolic calorimeter, the heat transfer will be mostly by conduction, hence P_{R} will be small and negligible compared with P_{C}.

The pressure terms in Eq. (A.4) are bolded to minimize confusion with any power terms. Under normal constant current (I) operation, the terms T, E, ΔT, and $\mathbf{P}$ will vary with time, t. The change of the cell temperature with time, as given by P_{calor} in Eq. (A.2), makes Eq. (A.1) a nonlinear, inhomogeneous differential equation. Although this differential equation can be used directly, numerical integration yields more accurate results (see Fig. 2). The P_{calor} term is obviously larger when the cell temperature is changing more rapidly such as when D_2O is replenished or when the internal heater is turned on (t_1) or off (t_2). The small progressive decrease with time for the cell temperature (Table 2) is due to the progressive increase of the electrolyte concentration due to electrolysis resulting in an increasing ionic conductance and hence a decreasing cell voltage and input power (Eq. (A.3)) as shown in Table 2.

The most complicated term, P_{gas}, is generally small except when the cell temperature exceeds 70°C. The electrolysis reaction

$$0.5\text{D}_2\text{O}_{(\text{l})} \rightarrow 0.5\text{D}_{2(\text{g})} + 0.25\text{O}_{2(\text{g})} \tag{A.8}$$

consumes 0.5 mol of D_2O and produces 0.5 mol of D_2 gas and 0.25 mol of O_2 gas per Faraday, F (96485.3415 C mol^{-1}). The 0.75 mol total of electrolysis gases generated per Faraday also carry away D_2O vapor due to the equilibrium vapor pressure of D_2O in the cell, $\mathbf{P} = \mathbf{P}_{\text{D}_2\text{O(g)}}$. Using Dalton's law of partial pressures, the moles of D_2O(g) carried away per Faraday are given by

$$\text{moles D}_2\text{O(g)} = 0.75(\mathbf{P}/(\mathbf{P}_{\text{D}_2} + \mathbf{P}_{\text{O}_2})) = 0.75(\mathbf{P}/(\mathbf{P}^* - \mathbf{P})), \tag{A.9}$$

where the gas pressure within the cell, $\mathbf{P}^*$, is expressed by

$$\mathbf{P}^* = \mathbf{P}_{\text{D}_2\text{(g)}} + \mathbf{P}_{\text{O}_2\text{(g)}} + \mathbf{P}_{\text{D}_2\text{O(g)}} \tag{A.10}$$

and is close to the atmospheric pressure for this open system. This $\mathbf{P}^*$ term dictates the monitoring of the atmospheric pressure for highly accurate calorimetric measurements, but this has not been done by most laboratories. The largest term for P_{gas} results from the large enthalpy of vaporization of D_2O, L =41678.9 J/mol at 101.42°C. Therefore, simpler versions of Eq. (A.4) are often used such as

$$P_{\text{gas}} = -(0.75I/F)(\mathbf{P}/(\mathbf{P}^* - \mathbf{P}))[(C_{p,\text{D}_2\text{O(g)}}\text{–}C_{p,\text{D}_2\text{O}(l)})\Delta T + L]. \tag{A.11}$$

Assuming $I = 0.2000$ A and $T_{\text{b}} = 22.00$°C, the P_{gas} term is −5.6489 mW at $T = 40.00$°C and increases to −57.8253 mW at $T = 80.00$°C. The term involving the enthalpy of vaporization (L) contributes −4.9103 mW (86.92%) and −52.9857 mW(91.63%), respectively, at these two cell temperatures. The electrolysis of D_2O in the calorimeter causes the equivalent moles (M) to change with time

$$M = M^\circ\text{–}(1 + \beta)\gamma It/2F), \tag{A.12}$$

where I is the constant current, β is the fraction of D_2O lost by evaporation, and γ is the current efficiency for electrolysis. Thus, a more exact expression used in earlier publication by Fleischmann and Pons is

$$P_{\text{calor}} = C_p \mathrm{d}/\mathrm{d}t\,(M\Delta T) = C_p M(\mathrm{d}\Delta T/\mathrm{d}t) + C_p \Delta T(\mathrm{d}M/\mathrm{d}t) \tag{A.13}$$

or equivalently

$$\begin{aligned} P_{\text{calor}} = {} & C_p[M^\circ - (l+\beta)\gamma It/2F](\mathrm{d}\Delta T/\mathrm{d}t) \\ & - C_p \Delta T(l+\beta)\gamma I/2F, \end{aligned} \tag{A.14}$$

where $\Delta T = T - T_b$. For constant T_b, $d\Delta T/\mathrm{d}t = \mathrm{d}T/\mathrm{d}t$. Except for small cells and large currents, the simpler Eq. (A.2) is adequate.

In chemical kinetics, the differential equations for the rates of the reactions are seldom used because the integrated expressions are much more accurate. The use of numerical integration of the calorimetric data also results in greater accuracy. Integrals can be numerically evaluated by using the mean value of the function and the integration limits. Mathematically,

$$\int_a^b f(x)\mathrm{d}x = (b-a)\langle f(x)\rangle, \tag{A.15}$$

where a and b are the integration limits and $\langle f(x)\rangle$ is the mean value of the function. Other approximate integration methods can also be used such as Simpson's Rule or the Trapezoidal Rule, but only Eq. (A.15) is, strictly speaking, correct in that it agrees with the mathematical definition of an integral. The Trapezoidal Rule, however, allows integration around the discontinuities at $t = t_1$ and $t = t_2$. The integrals of power over selected time periods give units of energy (J).

The required heat capacities at constant pressure (C_p), enthalpy of vaporization of D_2O (L), the vapor pressure of D_2O (**P**), and the thermoneutral potential (E_H) are available from thermodynamic tables at 25°C (298.15 K) and standard pressure. The temperature dependence of these calorimetric parameters at standard atmospheric pressure can be calculated from the following equations where T is the Kelvin temperature (°C + 273.15).

$$L = 85263.9 - 173.429T + 0.2586T^2 - 1.91913 \times 10^{-4}T^3 - 1805569T^{-1} \ \ (\text{in J/mol}^{-1}), \tag{A.16}$$

$$E_H = 1.5318346 - 0.0002067(T - 273.15) \ \ (\text{in V}), \tag{A.17}$$

$$\begin{aligned} \log \mathbf{P} = {} & 35.47686 - 3343.93T^{-1} - 10.9 \log T + 0.0041645T \\ & + 9.14056/(197.397 - T) \ \ (\mathbf{P} \text{ in atm}), \end{aligned} \tag{A.18}$$

$$\begin{aligned} C_{p,D_2O_{(l)}} = {} & 200.13 - 495.9 \times 10^{-3}T + 573.07 \times 10^{-6}T^2 \\ & - 16.765 \times 10^5 T^{-2} (\text{in J mol}^{-1}\text{K}^{-1}), \end{aligned} \tag{A.19}$$

$$\begin{aligned} C_{p,D_2O_{(g)}} = {} & 26.7006 + 21.2897 \times 10^{-3}T + 2.66774 \times 10^{-6}T^2 \\ & + 1.2907 \times 10^5 T^{-2} (\text{in J mol}^{-1}\text{K}^{-1}), \end{aligned} \tag{A.20}$$

$$\begin{aligned} C_{p,D_{2(g)}} = {} & 28.9778 - 1.49226 \times 10^{-3}T + 4.14779 \times 10^{-6}T^2 \\ & + 0.26544 \times 10^5 T^{-2} (\text{in J mol}^{-1}\text{K}^{-1}), \end{aligned} \tag{A.21}$$

$$\begin{aligned} C_{p,O_{2(g)}} = {} & 23.1436 + 18.2628 \times 10^{-3}T - 6.605 \times 10^{-6}T^2 \\ & + 1.2118 \times 10^5 T^{-2} (\text{in J mol}^{-1}\text{K}^{-1}). \end{aligned} \tag{A.22}$$

At a typical cell temperature of 60°C (333.15 K) and standard pressure, these calculated values are $L = 43672$ J mol^{-1}, $E_H = 1.5194V$, $\mathbf{P} = 0.18317$ atm, $C_{p,D_2O_{(l)}} = 83.420$ J mol^{-1}K^{-1}, $C_{p,D_2O_{(g)}} = 34.660$ J mol^{-1}K^{-1}, $C_{p,D_{2(g)}} = 29.180$ J mol^{-1}K^{-1}, and $C_{p,O_{2(g)}} = 29.587$ J mol^{-1}K^{-1}.

Equations (A.16)–(A.22) look daunting, but they can be handled readily by computers (Excel). These equations, along with Eqs. (A.2)–(A.7), were always used with the China Lake calorimetry [18].

Appendix A2. List of Symbols

C_p	Heat capacity at constant pressure, JK^{-1}mol^{-1}
E	Cell potential, V
E_H	Thermoneutral potential, V
F	Faraday constant, 96 485.3415 C mol^{-1}
I	Cell current, A
k_C	Conductive heat transfer coefficient, WK^{-1}
k'_C	Pseudo-conductive heat transfer coefficient, WK^{-1}
k_R	Radiative heat transfer coefficient, WK^{-4}
L	Enthalpy of evaporation for D_2O, J mol^{-1}
n_g	Moles of electrolysis gases, mol
M	Water equivalent of the calorimetric cell, mol
$\boldsymbol{P}$	Partial pressure of D_2O, Pa
$\mathbf{P}^*$	Atmospheric pressure, Pa
P_C	Power transferred by conduction, W
P_{calor}	Rate of enthalpy change within the calorimeter, W
P_{EI}	Power input due to electrolysis, W
P_{gas}	Rate of enthalpy transport by the gas stream, W
P_H	Power input due to the calibration heater, W
P_R	Power transferred by radiation, W
P_W	Rate of pressure–volume work by the generated gases, W
P_X	Excess power generated, W
R	Gas constant, 8.314472 JK^{-1} mol^{-1}
T_b	Temperature of water bath, K
T	Temperature of cell, K
ΔT	T–T_b, K
$f(T)$	$T^4 - T_b^4$, K^4
β	Fraction of D_2O lost by evaporation, dimensionless
γ	Current efficiency for electrolysis, dimensionless

References

[1] M.H. Miles, K.H. Park, D.E. Stillwell, *J. Fusion Energy* **9** (1990) 333.
[2] M.H. Miles, K.H. Park, D.E. Stilwell, *J. Electroanal. Chem.* **296** (1990) 409.
[3] M.H. Miles, B.F. Bush, D.E. Stilwell, *J. Phys. Chem.* **98** (1994) 1948.
[4] M.H. Miles, *J. Electroanal. Chem.* **482** (2000) 55.
[5] M.H. Miles, M. Fleischmann, M.A. Imam, Calorimetric Analysis of a Heavy Water Electrolysis Experiment Using a Pd-B Alloy Cathode, NRL/MR/6320-01-8526, March 26, 2001.
[6] M. Fleischmann, S. Pons, M.W. Anderson, L.J. Li, M. Hawkins, *J. Electroanal. Chem.* **287** (1990) 293.

[7] M. Fleischmann, M.H. Miles, *Proceeding of ICCF-10*, P.L. Hagelstein, S.R. Chubb (eds.), Cambridge, 2003, pp. 247–268.
[8] M.H. Miles, M. Fleischmann, *Low-Energy Nuclear Reactions Sourcebook*, J Marwan, S.B. Krivit (eds.), ACS Symposium Series, Vol. 998, 2008, pp. 153–171.
[9] M.H. Miles, M. Fleischmann, Proceedings of ICCF-14, Washington DC, 2008, submitted.
[10] D.A. Kidwell, K. Grabowski, NRL, Email communications. Note: We have not been able to obtain any experimental evidence from NRL that supports their claim for shuttle reactions, 2009.
[11] F.V. Andrade, L.J. Deiner, H. Varela, J.F.R. de Castro, I.A. Rodrigues, F.C. Nart, *J. Electrochem. Soc.* **154** (2007) F159.
[12] M.H. Miles, J.R. Alston, A.J. Davenport, A.A. Grumet, Low Melting Electrolytes for Thermal Batteries, SBIR Phase I Final Report, October 31, 2007.
[13] M.H. Miles, Chloride-Free Thermal Batteries Using Molten Nitrate Electrolytes, U.S. Patent No. 7,629,075 B2, December 8, 2009.
[14] M.H. Miles, *ICCF-15 Proceedings*, Rome, Italy, ENEA (ed.), 2009, submitted.
[15] D. Knies, NRL, E-mail communication, 2009.
[16] M.H. Miles, Chemical and Electrochemical Studies of Co-Deposition Systems in H_2O and D_2O, American Chemical Society Meeting, San Francisco, CA, March 21–25, 2010, in Preparation.
[17] M.H. Miles, M. Fleischmann, *ICCF-15 Proceedings*, Rome, Italy, ENEA (ed.), 2009, submitted.
[18] M.H. Miles, B.F. Bush, K.B. Johnson, Anomalous Effects in Deuterated Systems, NAWCWPNS TP 8302, September, 1996.